# Cascade Brillouin scattering as a mechanism for photoluminescence from rough surfaces of noble metals

V. Yu. Shishkov,[1,2,3] E. S. Andrianov,[1,2,3] A. A. Pukhov,[1,2,3] A. P. Vinogradov,[1,2,3] S. N. Orlov,[4] Yu. N. Polivanov,[4] V. I. Fabelinsky,[4] D. N. Kozlov,[4] V. V. Smirnov,[4] and A. A. Lisyansky[5,6]

[1]*Dukhov Research Institute of Automatics (VNIIA), 22 Sushchevskaya, Moscow 127055, Russia*
[2]*Moscow Institute of Physics and Technology, 9 Institutskiy per., Dolgoprudny 141700, Moscow reg., Russia*
[3]*Institute for Theoretical and Applied Electromagnetics, 13 Izhorskaya, Moscow 125412, Russia*
[4]*Prokhorov General Physics Institute of the Russian Academy of Sciences, Vavilov str. 38, 119991 Moscow, Russia*
[5]*Department of Physics, Queens College of the City University of New York, Flushing, New York 11367, USA*
[6]*The Graduate Center of the City University of New York, New York, New York 10016, USA*

(Received 28 July 2020; revised 9 December 2020; accepted 21 December 2020; published 11 January 2021)

In surface-enhanced Raman-scattering experiments that use plasmonic nanostructures as substrates, the scattering spectrum contains a broad background usually associated with photoluminescence. This background exists above and below the frequency of the incident wave. The low-frequency part of this background is similar to the scattering spectrum of a plasmon nanoparticle, while the high-frequency part follows the Gibbs distribution. We develop a theory that explains experimentally observed features in both the high- and low-frequency parts of the photoluminescence spectrum from a unified point of view. We show that photoluminescence is attributed to the cascade Brillouin scattering of the incident wave by metal phonons under the plasmon resonance conditions. The theory is in good agreement with our measurements over the entire frequency range of the background.

DOI: 10.1103/PhysRevB.103.035408

## I. INTRODUCTION

The term photoluminescence (PL) is commonly used for all types of light scattering, for which spectrum is much broader than the spectrum of incident radiation. PL of noble metals was first discovered back in 1969 [1] and was associated with a broad scattering spectrum resulting from incident argon-ion laser light ranging from 457.9 to 514.5 nm and from Hg-arc lamp light continuously ranging from 300 to 400 nm. The first phenomenological theory of PL of noble metal nanostructures was put forward in Ref. [2] and subsequently developed in Refs. [3–5]. In this theory, it is assumed that PL is associated with the radiative *interband* recombination of *sp* electrons and *d* holes. Before recombining with a *d* hole, an *sp* electron may lose energy due to *intraband* transitions. The mechanism is now referred to as Raman scattering on electrons in metals.

Interest in PL has been boosted due to the widespread use of surface-enhanced Raman spectroscopy (SERS). In SERS, the analyte is on a noble metal substrate. The metal substrates can be made as an assembly of individual particles or as granular or corrugated surfaces. Special studies of such structures [6,7] show that the reflection spectrum of both a single particle [8,9] and a substrate made of granular plasmonic nanostructures [1,2] have a broad frequency line. The broad frequency line is observed both below and above the frequency of the incident wave and is also referred to as PL. The integrated intensity of nanostructure photoluminescence (NSPL) strongly depends on the geometry of the plasmon nanostructure. For smooth metal surfaces, the NSPL intensity is extremely small. It is on the order of $10^{-10}$ smaller than the intensity of incident radiation. For granular substrates consisting of subwavelength spherical particles, this ratio is about $10^{-6}$, and for ellipsoid particles, it is on the order of $10^{-4}$ [2]. Since the Raman signal is very weak, NSPL may affect the results of Raman-scattering measurements. The need to separate these two effects has inspired the studies of PL of nanostructures made of noble metals [8–10].

A detailed experimental study [2,6,7,9] has shown that NSPL of noble metal structures differs from the usual PL considered in Ref. [1]. First, in contrast to conventional luminescence, NSPL is even observed when the frequency of incident light, $\omega_0$, is lower than the frequencies of interband electron transitions [2,9], which, according to Ref. [1], are responsible for PL in metals. Second, the shapes of the NSPL spectra, $S_{\mathrm{NSPL}}(\omega)$, are different above $\omega > \omega_0$, and below $\omega < \omega_0$, the frequency of the incident wave. Specifically, above $\omega_0$, the NSPL intensity decreases with an increasing frequency $\omega$ according to the Gibbs distribution $\exp(-\hbar(\omega-\omega_0)/k_BT)$ [9]. Moreover, in the high-frequency part spectrum, the NSPL intensity increases with temperature [9]. Below $\omega_0$, $S_{\mathrm{NSPL}}(\omega)$ is close to the *scattering spectrum for a plasmon nanostructure* (SSPNS), $S_p(\omega)$. This dependence arises when a plasmon structure is illuminated by a wave having a continuous white spectrum. The latter case was realized in Ref. [6], where plasmon nanoparticles were illuminated by short pulses.

It is natural to connect NSPL with the plasmon resonance of the roughness of a "smooth" surface of a nanostructure [6,7,11–13]. The elastic scattering of the incident wave on

 

a nanostructure is usual Rayleigh scattering, which spectrum should coincide with the spectrum of incident radiation. However, NSPL excited by laser light has a broad spectrum whose shape is close to the SSPNS of the nanostructure. In particular, the NSPL spectrum has a maximum at the frequency close to the plasmonic resonance frequency. Thus, NSPL cannot be reduced to elastic scattering [9].

In Refs. [6,9], as an inelastic process, the *intraband* transitions of electrons inside the *sp* band is considered. Since *intraband* dipole transitions are forbidden, the theory of Ref. [9], similar to Raman scattering, introduces a virtual level to which an electron can be excited by capturing a photon and then returning back. The process is considered as a creation of an electron-hole pair. To explain the Gibbs dependence of the high-frequency part of the spectrum, the following process has been employed. An electron thermally excited above the Fermi level absorbs the incident photon and gets excited to a virtual level. Then, this electron emits a plasmon and falls in an empty *state* slightly below the Fermi level. Since the states in the *s* band are not all filled, in contrast to the *interband* transitions, where the hole energy is fixed, the electron has the opportunity to relax into a state with higher or lower energy, violating the elasticity of the process. The similarity of NSPL and the SSPNS has been explained by the fact that an excited electron-hole pair recombines emitting a plasmon. This explanation is in qualitative agreement with experiment. Also, the Gibbs distribution of the number of electrons above the Fermi level explains the temperature dependence of the NSPL intensity in the high-frequency spectrum.

Although the consideration, based on the *intraband* transitions in the *sp* band, qualitatively describes the plasmon resonant shape, to describe the low-frequency part of the NSPL spectrum and temperature dependence, an existence of an artificial virtual level has to be assumed.

In this paper, we propose a mechanism for the NSPL spectrum formation that is not based on interband transitions. To describe experiments, we use the recently developed approach [14–16], which we have used to explain the inelastic Raman scattering [16]. In this approach, the direct interaction of driven oscillations of molecular electrons with vibrations of nuclei in a molecule is taken into account [14–16]. We extend this approach to the Brillouin scattering by taking into account the direct interaction of a driven oscillation of electrons in a metallic nanoparticle with phonons. This interaction is described by the optoacoustical Hamiltonian [14,17–19]. The spontaneous Brillouin scattering of the electromagnetic (EM) field caused by this oscillation excites an oscillation of the EM field inside the nanoparticle at a shifted frequency (the Stokes shift). The field at the shifted frequency also undergoes Brillouin scattering launching the cascade of Brillouin scattering processes of an EM field inside the nanoparticle. The frequency of each new oscillation is shifted by the Stokes shift. Such a cascade process continues as long as the frequency of a new oscillation falls into the SSPNS. In the Stokes part of the spectrum, the developed theory reproduces the SSPNS. We also show that the Gibbs distribution of the high-frequency intensity is due to the anti-Stokes Brillouin scattering. All these effects are explained within a unified approach, without separate considerations of high- and low-frequency components. The theory is in good agreement with our measurements made over the entire frequency range of the background.

## II. PHOTOLUMINESCENCE SPECTRA FROM AU STOCHASTIC NANOSTRUCTURED FILMS: EXPERIMENT

To compare the results of the developed theory with experiment, we obtain our own experimental data because, for the same sample, measurements have mainly been obtained either for the high- or low-frequency parts of the spectrum [7,9,10]. As far as we know, the only measurements for the whole frequency range of the NSPL spectrum are only presented in Refs. [9,20]. However, in Ref. [9], the frequency of the incident EM field is exactly equal to the plasmon resonance frequency. The spectra presented in Ref. [20] look qualitatively similar to ours. However, the experiment of Ref. [20] and the theory developed in Refs. [20,21] are not devoted to studying PL but to study the effect of electrons of a metal particle on the Raman spectrum of an analyte molecule adsorbed by the particle. Therefore, the spectra obtained in the present paper are more comprehensive, allowing for a more detailed comparison with the theory.

In this section, we provide the results of the measurements of PL of granular gold films. The results are obtained for the entire spectrum of NSPL for different relations between the incident field frequency and the plasmon resonance frequency for the same nanoparticle. We use randomly nanostructured Au film (MATO S, manufactured by AtoiID, Lithuania, http://atoid.com). The stochastic nanopattern of a 200-nm-thick Au film is formed by magnetron sputtering of the metal to an ultrashort laser pulse ablated soda-lime-silica glass substrate. To demonstrate the random character of the surface structure, scanning electron microscopy (SEM) images of two different fragments of a Au film surface are presented in Fig. 1 with the length scale indications of 500 nm and 5 $\mu$m. Features from a few tens of nanometers to almost a micrometer in size are observed. Atomic force microscope (AFM) pictures of the surface show that its average roughness can be estimated as 0.4 $\mu$m. The samples provide distinct surface plasmon resonance characteristics for various excitation wavelengths.

To record PL spectra, a scanning confocal laser Raman microspectrometer ("Confotec CARS," SOL Instruments Ltd., Belarus) was used. The system, operating in the Sector of Raman Spectroscopy of Joint Institute for Nuclear Research (Dubna, Russia), was described in detail in Ref. [22]. Briefly, a 10-mW cw beam of 633-nm He-Ne excitation laser (05-LHP-991, Melles-Griot) was focused onto the sample using an inverted microscope with a 40×/0.6 numerical aperture lens (the focal depth $\sim$1.6 $\mu$m), providing the focal spot of $\approx$1-$\mu$m diameter. The scattered radiation, propagating in the backward direction, was collected by the objective, spectrally filtered within an appropriate range, and directed to the entrance slit of a 520-mm focal length grating spectrograph (MS 5004i, Solar TII, Belarus), with a 150 grooves/mm grating in the first order (the dispersion 12.6 nm/mm enables one to cover the Raman shift range of $\approx\pm 3000\,\mathrm{cm}^{-1}$). The spectra were recorded by a cooled 2048 × 122-elements, 12 $\mu$m × 12 $\mu$m each, 16-bit analog to digital converter charge-coupled device (CCD) array photodetector (HS 101H, PROSCAN, Belarus) working in the "full vertical binning" mode, i.e., as a linear array. The

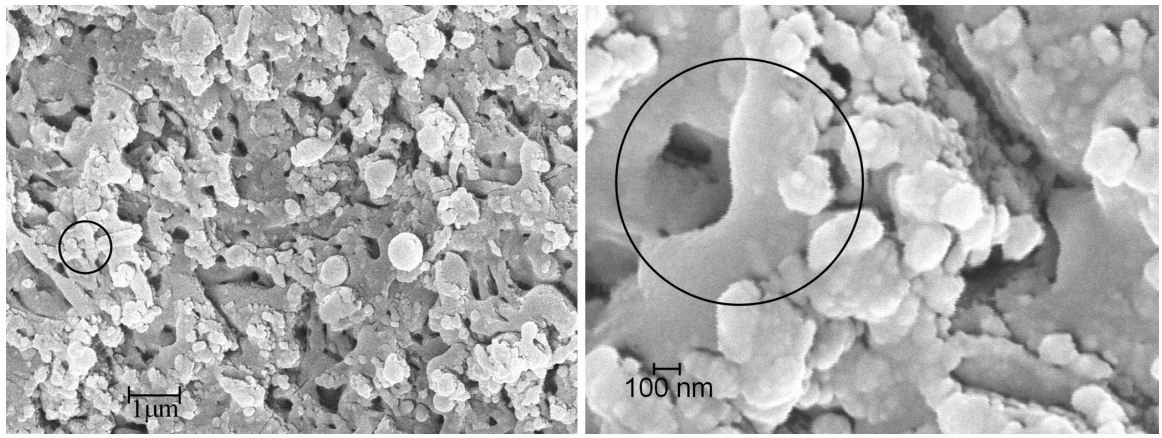


FIG. 1. SEM images of the Au film surface area fragments of different scales. The black circles show 1-$\mu$m excitation laser beam spots at the surface.

radiation was accumulated by the CCD array during the preset exposure time of 3 s. To record the spectra simultaneously in both Stokes and anti-Stokes regions, a notch filter (StopLine single-notch filter, Semrock) was used to suppress the excitation radiation with the coefficient of suppression $>10^6$.

In Fig. 2, the thin blue lines represent PL spectra recorded from an $\sim$1 $\mu$m spatial point of the nanostructured Au surface at three different excitation intensities: 39, 75, and 150 $\mu$W/$\mu$m$^2$. One can clearly see the dip of $\sim$600-cm$^{-1}$ width, provided by the notch filter near the excitation wavelength. Here, the spectral profiles are corrected for the detection system spectral efficiency, evaluated using the transmission curves of the optical elements, the grating diffraction efficiency, and the CCD quantum efficiency. These profiles represent the relative flux of scattered radiation $I$ in photons/s. The position of the broad peak in the Stokes region varies within the range of about 500 cm$^{-1}$. The anti-Stokes part of the spectrum is approximated as $I \sim \exp(-h(\omega-\omega_0)/k_BT)$, with the temperature $T \approx 330$ K.

## III. QUALITATIVE DESCRIPTION OF THE CASCADE BRILLOUIN PROCESS

In the external EM field, electrons and phonons form a closed quantum system without dissipation. In such a system, the incident field leads to the emergence of complex dynamics of the energy exchange inside but cannot cause radiation. Therefore, to describe light emission, we must take into account the interaction of the closed system with a reservoir of free-space modes [23–25].

Below, we solve the problem of PL from plasmonic nanostructures in two stages. First, we introduce the dissipation terms corresponding to the interaction of the system with an unperturbed reservoir of free-space modes [26] and find the behavior of the system and then determine the changes in the reservoir states caused by this behavior. Second, in the framework of the dipole approximation of the classical electrodynamics [27] (see also Appendix D), we consider the interaction of the quasiparticles with the reservoir of free-space modes.

As an inelastic mechanism leading to NSPL, we consider Brillouin scattering. A laser beam induces an EM field inside a plasmonic nanoparticle. We assume that the size of the nanoparticle is smaller than the skin depth. Consequently, the driven oscillations of the electric field inside the particle are uniform. Due to Brillouin scattering of this field, the EM field at the Stokes frequency appears. The frequency of this field is shifted by the phonon frequency. Because the latter is small compared to the width of SSPNS, the frequency of this excited field lies within the SSPNS.

The oscillations of the EM field caused by the incident wave and the scattered field cause the oscillations of electron density in metal and, consequently, the oscillations of the metal nuclei. Since the beat frequency of these fields coincides with the phonon frequency, the number of phonons resonantly increases, causing the increase in Brillouin scattering and in the intensity of the Stokes field. An increase in the number of quanta in the Stokes field, $n(\omega_{\rm St})$, is determined by two processes. The first one is the stimulated excitation like that in the stimulated Raman scattering (SRS) [28], which is equal to $G_\downarrow n(\omega_{\rm St})n(\omega_0)$. Here $G_\downarrow$ denotes the rate of the increase in the intensity of the Stokes component (the symbol $\downarrow$ indicates the process in which the EM field with the lower frequency is excited by the field with the higher frequency–the Stokes process). The second process is the spontaneous Brillouin scattering, caused by vacuum zero-point vibrations with the Stokes frequency. This process is analogous to the excitation of the Stokes field in the Raman laser operating below the threshold. The rate of this process is $G_\downarrow n(\omega_0)$ [28]. Thus, the incident wave pumps the oscillation at the Stokes frequency, and the energy is accumulated in the EM field at the Stokes frequency. The dynamics of the Stokes intensity may be described by the rate equation

$$\dot{n}(\omega_{\rm St}) = -\gamma_{\rm rad}(\omega_{\rm St})n(\omega_{\rm St}) + G_\downarrow n(\omega_0)(n(\omega_{\rm St})+1) \qquad (1)$$

where $\gamma_{\rm rad}(\omega_{\rm St})$ is the rate of losses determining the width of the SSPNS. We can estimate the stationary value of $n(\omega_{\rm St})$ as $n(\omega_{\rm St}) \sim G_\downarrow n(\omega_0)/\gamma_{\rm rad}(\omega_{\rm St}) \ll 1$. Since $n(\omega_{\rm St}) \ll 1$, the process of the spontaneous Brillouin scattering is much more intense than the stimulated emission.

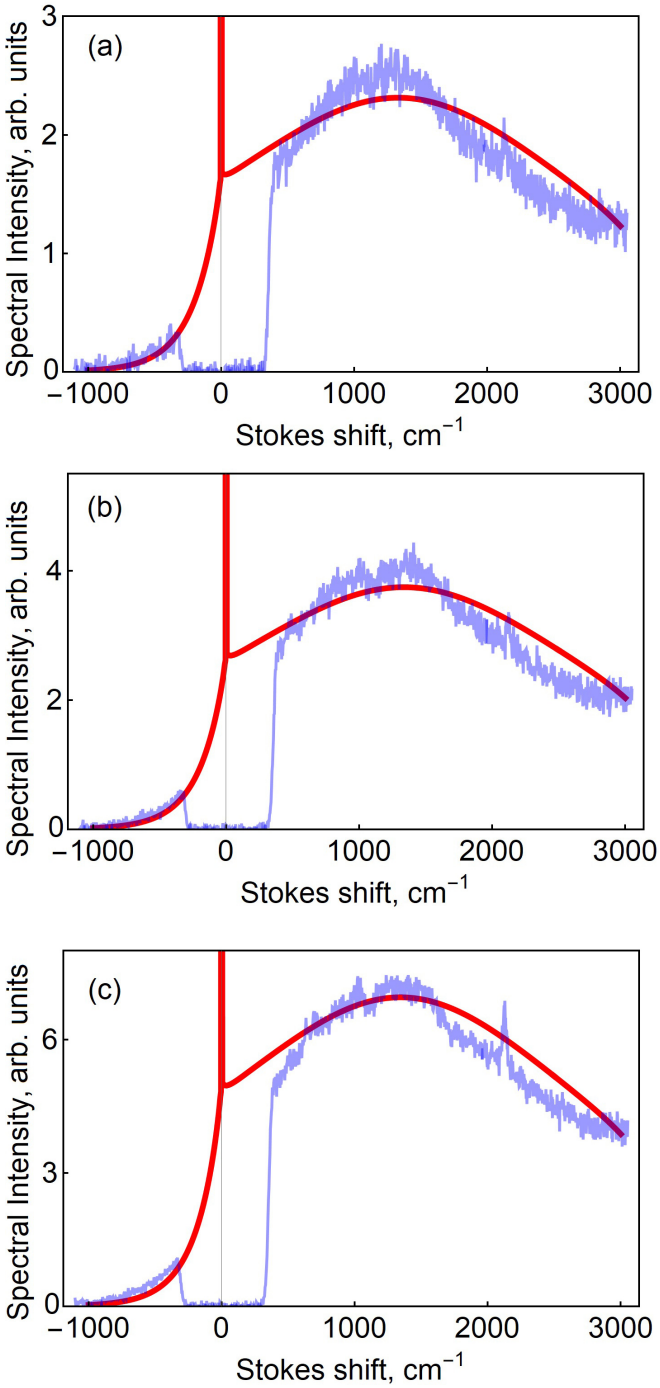


FIG. 2. The dependence of the intensity of scattered light (in arbitrary units) on the wavelength at pump rates of (a) 39 $\mu$W, (b) 75 $\mu$W, and (c) 150 $\mu$W. The experimental results are shown by the thin blue lines; the theoretical curves shown by the thick red lines are obtained by numerical calculations of Eqs. (2)–(4) and (12). Zero on the horizontal axis corresponds to the wavelength of the incident light (633 nm).

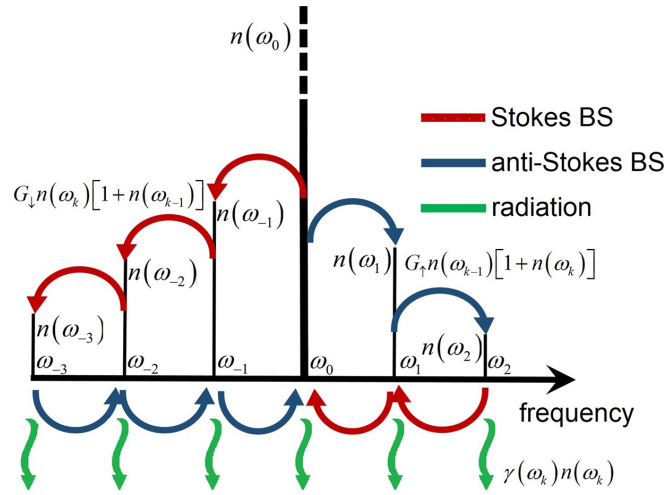


FIG. 3. The schematic of the interaction between the driven oscillations of the electric field at various frequencies inside the nanoparticle. The $k$ th driven oscillation dissipates with the rate $\sim\gamma(\omega_k)n(\omega_k)$ (wavy green lines) and exchanges the energy with the nearby driven oscillation at higher (blue lines) at lower (red lines) frequencies. The rates of corresponding exchanges of the energy are $G_\uparrow n(\omega_k)[1+n(\omega_{k+1})]$ and $G_\downarrow n(\omega_k)[1+n(\omega_{k-1})]$, respectively.

The term $G_\downarrow n(\omega_{\rm St})n(\omega_0)$ can be expressed in a more standard form by using nonlinear susceptibility $\chi^{(3)}$. Namely, if instead of the number of quanta $n(\omega_{\rm St})$, we consider the dynamics of the *intensity* of the field at the Stokes frequency, $I(\omega_{\rm St})$, then the rate of the stimulated Brillouin scattering has the form $\sim{\rm Im}\chi^{(3)}I(\omega_{\rm St})I(\omega_0)$. The constants $G_\downarrow$ and $\chi^{(3)}$ are related by $G_\downarrow \approx {\rm Im}\chi^{(3)}\hbar\omega^2/V$.

As we see, the spontaneous Brillouin scattering gives the main contribution to the process of PL. For this reason, we use the notation $G_\downarrow$ instead of $\chi^{(3)}$ to avoid the misleading association of PL with the stimulated process.

As we show, NSPL occurs due to a cascade of driven oscillations of the EM field inside the nanoparticle at different frequencies. Thus, we consider the nanoparticle as a resonator having the same line function shape as the SSPNS. Therefore, the incident field causes a driven oscillation of the field inside the nanoparticle with the frequency of the incident wave, $\omega_0$, and is accompanied by the oscillation of the dipole moment of the nanoparticle. That leads to Rayleigh scattering of the incident wave.

In Brillouin scattering, the Stokes shift is usually much smaller than the plasmon resonance linewidth. A *single* process, therefore, cannot explain the shape of the NSPL spectrum. To understand where the broad shape of NSPL comes from, one should take into account that the stationary Stokes field excites the next oscillations at the frequencies displaced by the same Stokes shift, $\omega_{\rm ph}$, with respect to the Stokes frequency $\omega_0-\omega_{\rm ph}$. In turn, the EM field at the frequency $\omega_0-\omega_{\rm ph}$ excites the field at the frequency $\omega_0-2\omega_{\rm ph}$, which then excites the field at the frequency $\omega_0-3\omega_{\rm ph}$, and so on. These processes form a cascade of oscillations at frequencies inside the SSPNS (indicated by red arrows in Fig. 3, in which the cascade process is shown schematically).

We enumerate oscillations with the subscript $k$. The frequencies of single anti-Stokes and Stokes shifts are $\omega_1\equiv\omega_{\rm aSt}=\omega_0+\omega_{\rm ph}$ and $\omega_{-1}\equiv\omega_{\rm St}=\omega_0-\omega_{\rm ph}$, respectively, the frequencies of double anti-Stokes and Stokes shifts are $\omega_2\equiv\omega_{\rm aSt}+\omega_{\rm ph}=\omega_0+2\omega_{\rm ph}$ and $\omega_{-2}\equiv\omega_{\rm St}-\omega_{\rm ph}=\omega_0-2\omega_{\rm ph}$, respectively, and so on. Thus, the frequency $\omega_k$ of the $k$ th

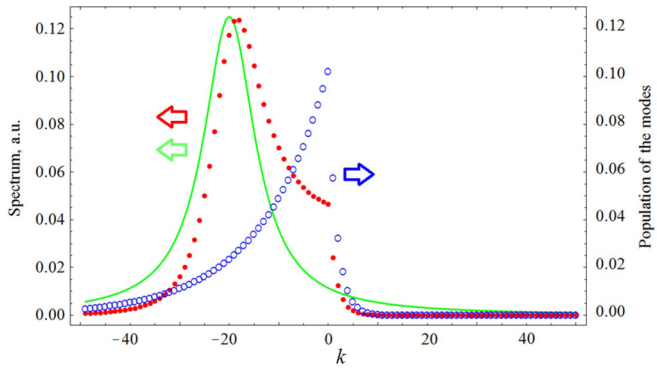


FIG. 4. The frequency dependencies of the quasiparticle population of the mode $n_n^{\rm st}$ (blue circles) and the quasiparticle radiation rate $\gamma_{\rm rad}(\omega_k)$ (solid green line) on the mode number. Red circles represent the dependence of the spectrum $S(\omega_n)$ on the frequencies $\omega_n$. System parameters are $\omega_0 = 633$ nm, $T = 300$ K, $\gamma/\omega_0 = 0.01$, $G_\downarrow/\omega_0 = 0.3$, $G_\uparrow = G_\downarrow \exp(-\Delta\omega/T) = 0.3G_\downarrow$, and $P/\omega_0 = 0.017$.

oscillation is $\omega_0 + k\omega_{\rm ph}$. The number of quanta in the $k$ th oscillation is denoted by $n(\omega_k)$.

The radiated intensity is proportional to the product of the squared dipole moment and the number of quanta. The dependence of $n(\omega_k)$ on $\omega_k$ (Fig. 4, blue circles) is obtained as a solution of generalized Eq. (1) extended on all energy exchanges shown in Fig. 3. The dependence of the dipole susceptibility of the nanoparticle on the frequency is determined by the plasmon resonance and has the Lorentzian shape (Fig. 4, green line). Therefore, the amplitude of the emission spectrum (Fig. 4, red circles) differs from the amplitude of the number of oscillation quanta (Fig. 4, blue circles) by the corresponding values of the green line. Taking into account the decay of oscillations and the dispersion factor with a resonant frequency dependence, we obtain the radiation spectrum with the maximum shifted toward the incident radiation frequency (the difference between the red circles and the green line in Fig. 4). This shift is observed in experiment [8].

Along with the excitation of the EM field at the Stokes frequency, the field is also excited at the anti-Stokes frequency (blue arrows in Fig. 3). This results in the energy flow from the field at the frequency $\omega_k$ to the field at the frequency $\omega_k + \omega_{\rm ph}$.

The qualitative description of the mechanism for NSPL of metals presented above does not take into account the cascade of anti-Stokes scatterings. Consequently, it does not describe the shape of the spectrum above the frequency of the incident EM field, resulting from such a cascade. For its description, a consistent quantum-mechanical approach is necessary. This description is developed in the next section.

## IV. QUANTUM-MECHANICAL EQUATIONS DESCRIBING CASCADE BRILLOUIN PROCESS

As we discussed in the previous section, the driven oscillation excited by the external field with the frequency $\omega_0$ is amplified due to the closeness of $\omega_0$ to $\omega_{\rm pl}$. Due to the nonlinear Brillouin scattering, the EM field of this driven oscillation with the frequency $\omega_0$ induces the next driven oscillation with the frequency $\omega_0 - \omega_{\rm ph}$. We denote the complex amplitude of a driven oscillation at the frequency $\omega_k$ as $a(\omega_k, t)$.

Brillouin scattering also contributes to the fields at anti-Stokes frequencies. Thus, there is a process of energy redistribution among the driven oscillations. To describe the dynamics of the cascade Brillouin energy transport in NSPL, we should consider the quantum properties of the phenomena.

For this purpose, we use the procedure of macroscopic quantization [29,30] that includes quantization of the EM field and collective electron oscillations in the plasmon structure, as well as the modes of reservoirs with which these electrons interact. Such reservoirs can be phonons, impurities, etc. This theory relies only on the general linear properties of the medium (the linear permittivity) and does not require complicated first-principle calculations. A detailed derivation of the system Hamiltonian is given in Appendix A. The eigenmodes of such a system are collective oscillation states of electrons and reservoir modes. The eigenmodes (quasiparticles) can be found by using the Fano diagonalization procedure [26,29,30]. For each quasiparticle at the frequency $\omega_k$, we introduce annihilation and creation operators, $\hat{a}(\omega_k, t)$ and $\hat{a}^\dagger(\omega_k, t)$. The mean values of these operators have the meaning of dimensionless complex amplitude of oscillations of eigensolution at the frequency $\omega_k$. The operator of the number of quasiparticles is determined in the usual way as $\hat{n}(\omega_k, t) = \hat{a}^\dagger(\omega_k, t)\hat{a}(\omega_k, t)$. The mean value of this operator has the meaning of the dimensionless energy of oscillations. The closer the frequency of a quasiparticle to the plasmon resonance frequency, the greater the dipole moment of this quasiparticle. As shown in Appendix A, the frequency dependence of the squared dipole moment of the quasiparticle coincides with the SSPNS. Since it is the squared dipole moment that determines the ability of the quasiparticle to radiate, we can consider only quasiparticles which frequencies belong to the SSPNS.

In Appendix B, we show that the equations of motion for the expected values of operators $\langle\hat{a}(\omega_0, t)\rangle \equiv a(\omega_0, t)$, $\langle\hat{a}(\omega_k, t)\rangle \equiv a(\omega_k, t)$, and $\langle\hat{n}(\omega_k, t)\rangle \equiv n(\omega_k, t)$ have the form of the rate equations [24]:

$$\frac{da(\omega_0,t)}{dt} = (-i\omega_0 - \gamma_{\rm rad}(\omega_0)/2)a(\omega_0,t) - i\Omega_{\rm ex}\exp(-i\omega_0 t) + \frac{a(\omega_0,t)}{2}\sum_{m\neq 0}\left\{G_{\omega_m,\omega_0}n(\omega_m,t) - G_{\omega_0,\omega_m}[n(\omega_m,t)+1]\right\}, \quad (2)$$

$$\frac{da(\omega_k,t)}{dt} = (-i\omega_k - \gamma_{\rm rad}(\omega_k)/2)a(\omega_k,t) + \frac{a(\omega_k,t)}{2}\sum_{m\neq k}\left\{G_{\omega_m,\omega_k}n(\omega_m,t) - G_{\omega_k,\omega_m}[n(\omega_m,t)+1]\right\}, \quad k\neq 0, \quad (3)$$

$$\frac{dn(\omega_k,t)}{dt} = -\gamma_{\rm rad}(\omega_k)n(\omega_k,t) + \sum_m\left\{n(\omega_m,t)[n(\omega_k,t)+1]G_{\omega_m,\omega_k} - n(\omega_k,t)[n(\omega_m,t)+1]G_{\omega_k,\omega_m}\right\}, \quad k\neq 0, \quad (4)$$

where $\gamma_{\rm rad}(\omega_k)$ is the rate of radiative losses of the quasiparticle with the eigenfrequency $\omega_k$, $\Omega_{\rm ex} = -\mathbf{d}(\omega_0)\cdot\mathbf{E}_0/\hbar$ is the interaction constant between the external field with the amplitude $\mathbf{E}_0$ and the quasiparticle with the frequency $\omega_0$ and the dipole moment $\mathbf{d}(\omega_0)$. For the nanoparticle of the radius $R$, the dipole moment of the $k$ th quasiparticle is determined as

$$\mathbf{d}(\omega) = 4\pi R^3\sqrt{\frac{\Delta\omega\hbar\varepsilon_0}{\pi R^3}}\frac{\sqrt{{\rm Im}\varepsilon_{\rm M}^{\rm (lin)}(\omega)}}{\left|\hat{\varepsilon}_{\rm M}^{\rm (lin)}(\omega)+2\right|}\mathbf{e}_d,$$

where $\mathbf{e}_d$ is the unit vector in the direction of the dipole moment, and $\hat{\varepsilon}_{\rm M}^{\rm (lin)}(\omega) = {\rm Re}\varepsilon_{\rm M}^{\rm (lin)}(\omega) + i{\rm Im}\varepsilon_{\rm M}^{\rm (lin)}(\omega)$ is the linear part of metal permittivity.

Equations (2)–(4) have clear physical meaning. According to Eq. (2), the quasiparticle with the frequency $\omega_0$ is excited by the coherent external field with the same frequency and by incoherent fields of the other quasiparticles with frequencies $\omega_m$, $m\neq 0$. A quasiparticle with the frequency $\omega_{k\neq 0}$ is only excited by incoherent fields of the other quasiparticles with frequencies $\omega_{m\neq k}$, Eq. (3). The number of quasiparticles with $\omega_k$ is governed by rate equation (4). The quantity $n(\omega_k,t)$ up to the factor $\hbar\omega_k$ determines the total energy (coherent and incoherent) in the corresponding mode. Note that if in Eq. (4) we put $\omega_k = \omega_{\rm St}$, then in the sum, only the term with $m=0$ remains; then, replacing $G_{\omega_0,\omega_{\rm St}}$ by $G_\downarrow$, we obtain Eq. (1).

Equation (3) has a trivial stationary solution, $a(\omega_k,t) = 0$, $k\neq 0$. This solution indicates that quasiparticles with the frequencies $\omega_k\neq\omega_0$ are incoherent. When the condition $\sum_m\{G_{\omega_m,\omega_k}n(\omega_m,t) - G_{\omega_k,\omega_m}(n(\omega_m,t)+1)\} = \gamma_{\rm rad}(\omega_k)$ is fulfilled, there also may be a nontrivial stationary solution $a(\omega_k,t)\sim a^{st}(\omega_k)\exp(-i\omega_k t)$ with $a(\omega_k)\neq 0$, $k\neq 0$. This solution corresponds to the beginning of self-oscillations, which occur in a Raman laser with a high-$Q$ resonator [31,32]. When a plasmonic nanoparticle plays the role of the resonator, the beginning of self-oscillations only occurs at high-power pulse pumping [18]. Here, we do not consider such a situation and only deal with the case $a(\omega_k,t) = 0$, $k\neq 0$, which is relevant to our experiment.

The values $G_{\omega_m,\omega_k}$ are the rates of scattering of a quasiparticle from the state with the frequency $\omega_k$ to the state with the frequency $\omega_m$. The term $\sim G_{\omega_m,\omega_k}n(\omega_m,t)n(\omega_k,t)$ describes the process of the stimulated Brillouin excitation (like in SRS), while $\sim G_{\omega_m,\omega_k}n(\omega_m,t)$ describes the process of spontaneous excitation.

As mentioned in the Introduction, the intensity of Brillouin scattering on a metal surface is smaller by order of magnitude as compared to PL from a nanoparticle. The model developed in this section is quite general; it can be applied to Brillouin scattering on a metal surface. As it follows from Eqs. (A13) and (B6), the difference between scatterings from a surface and a nanoparticle is in the interaction constants, which is determined by the square of the overlapping integral of the electric-field distribution inside the metal, $\mathbf{\Lambda}_m^{(0)}(\mathbf{r})$, and the distribution of the phonon displacement, $C_l^*(\mathbf{r})$,

$$G_{\omega_m,\omega_n}\sim(w_{nml})^2 = \left(\tilde{w}_l\int_V d^3\mathbf{r}\mathbf{\Lambda}_n^{(0)*}(\mathbf{r})\mathbf{\Lambda}_m^{(0)}(\mathbf{r})C_l^*(\mathbf{r})\right)^2.$$

Since due to the normalization, both $\mathbf{\Lambda}_m^{(0)}(\mathbf{r})$ and $C_l(\mathbf{r})$ are inversely proportional to $\sqrt{V}$, from Eq. (A13) it follows that $w_{nml}\sim 1/\sqrt{V}$. If the nanoparticle's size $R$ is much less than both skin depth $\delta$ and the phonon coherence length $L_{\rm coh}$ ($R\ll\delta, L_{\rm coh}$), then the field and phonon distributions overlap in the entire volume of the nanoparticle, and the interaction constant $G_{\omega_m,\omega_n}$ does not depend on the skin depth and $L_{\rm coh}$. A different dependence arises when we consider Brillouin scattering on the metal surface. In this case, the field penetrates the metal within the skin depth $\delta\sim 30$ nm while phonons are coherent over the length $L_{\rm coh}\sim 10\ \mu$m, which is much less than the total volume of the metal. As a result, in the case of Brillouin scattering on a metal surface, the interaction between the electric-field modes $G_{\omega_m,\omega_n}$ differs by the factor $(w_{nml})^2\sim(\delta/L_{\rm coh})^2\sim 10^{-3}$ from Brillouin scattering in metal nanoparticles. This estimation can explain why the background of Brillouin scattering on a metal nanoparticle is much larger than that on the metal surface [9].

## V. PHOTOLUMINESCENCE SPECTRUM

Now we are ready to calculate the whole emission spectrum, $S(\omega)$, which includes both the NSPL spectrum, $S_{\rm NSPL}(\omega)$, and Rayleigh scattering, $S_{\rm R}(\omega)$, of a plasmon nanoparticle. As mentioned in Sec. III, we consider the formation of the PL background as a two-step process. At the first step, we suppose that the external field creates the stationary value of the number of quasiparticles. At the second step, we find the spectrum created by radiation of dipole moments of quasiparticles, which are in their stationary state. In Appendix D, we show that the spectrum can be expressed in the form (see also Refs. [25,33])

$$S(\omega) = \frac{1}{\pi}\hbar\omega t\sum_k\gamma_{\rm rad}(\omega_k)\int_{-\infty}^{+\infty}d\tau\langle\hat{a}^\dagger(\omega_k,t_{\rm st})\hat{a}(\omega_k,t_{\rm st}+\tau)\rangle\exp(i\omega\tau). \tag{5}$$

Now, we need to find two-time correlators $\langle\hat{a}^\dagger(\omega_0,t)\hat{a}(\omega_0,t+\tau)\rangle$ and $\langle\hat{a}^\dagger(\omega_k,t_{\rm st})\hat{a}(\omega_k,t_{\rm st}+\tau)\rangle$. To do this, we use the quantum regression theorem [25], which states that two-time correlators of an operator are described by the same equations as the one-time correlator. In our case, these correlators are governed by Eqs. (2) and (3), respectively. Assuming that $n(\omega_k,t)\ll 1$ and $\gamma_{\rm rad}(\omega_0)\gg G_{\omega_k,\omega_m}$ we obtain

$$\frac{d}{d\tau}\langle\hat{a}^\dagger(\omega_0,t)\hat{a}(\omega_0,t+\tau)\rangle = (-i\omega_0-\gamma_{\rm rad}(\omega_0))\langle\hat{a}^\dagger(\omega_0,t)\hat{a}(\omega_0,t+\tau)\rangle - i|a(\omega_0,t_{\rm st})|^2\Omega_{\rm ex}\exp(-i\omega_0\tau), \tag{6}$$

$$\frac{d}{d\tau}\langle\hat{a}^\dagger(\omega_k,t)\hat{a}(\omega_k,t+\tau)\rangle = (-i\omega_k-\gamma_{\rm rad}(\omega_k))\langle\hat{a}^\dagger(\omega_k,t)\hat{a}(\omega_k,t+\tau)\rangle,\quad k\neq 0. \tag{7}$$

The solutions to Eqs. (6) and (7) for $t \to +\infty$ are

$$\langle \hat{a}^\dagger(\omega_0, t_{\rm st})\hat{a}(\omega_0, t_{\rm st}+\tau)\rangle = \frac{-i\Omega_{\rm ex}|a(\omega_0, t_{\rm st})|^2}{\gamma_{\rm rad}(\omega_0)} \exp(-i\omega_0\tau), \tag{8}$$

$$\langle \hat{a}^\dagger(\omega_k, t_{\rm st})\hat{a}(\omega_k, t_{\rm st}+\tau)\rangle = n(\omega_k, t_{\rm st}) \exp[(-i\omega_k - \gamma_{\rm rad}(\omega_k))\tau], \quad k \neq 0. \tag{9}$$

To complete the calculations, we need to find $a(\omega_0, t_{\rm st})$ and $n(\omega_k, t_{\rm st})$. To calculate these quantities, we note that the energy transfer coefficient, $G_{\omega_m,\omega_k}$, is rather small, and we can assume that $n(\omega_k) \ll n(\omega_0)$ for any $k \neq 0$. For the stationary process when $t \gg t_{\rm st}$, we can neglect time derivatives in the left-hand side of Eqs. (2)–(4). Then, we find the equations for the stationary values of $a(\omega_0, t_{\rm st})$ and $n(\omega_k)$:

$$a(\omega_0, t_{\rm st}) = \frac{-i\Omega_{\rm ex}\exp(-i\omega_0 t)}{\gamma_{\rm rad}(\omega_0) + \sum_m G_{\omega_m,\omega_0}}, \tag{10}$$

$$-\gamma_{\rm rad}(\omega_k)n(\omega_k, t_{\rm st}) + \sum_m \left\{G_{\omega_k,\omega_m}n(\omega_m, t_{\rm st})[1 + n(\omega_k, t_{\rm st})] - G_{\omega_k,\omega_m}n(\omega_k, t_{\rm st})[1 + n(\omega_m, t_{\rm st})]\right\} = 0, \quad k \neq 0. \tag{11}$$

Equation (10) and the solution of Eq. (11) should be substituted to Eqs. (8) and (9), respectively.

Equation (7) contains both contributions of Rayleigh scattering, $S_{\rm R}(\omega)$, [see Eq. (8)] and of PL, $S_{\rm NSPL}(\omega)$, [see Eq. (9)]. Combining Eqs. (5) and (9) one can find the NSPL spectrum $S_{\rm NSPL}(\omega)$:

$$S_{\rm NSPL}(\omega) = \frac{1}{\pi}t\sum_{k\neq 0}\frac{\hbar\omega_k\gamma_{\rm rad}(\omega_k)}{\gamma_{\rm rad}^2(\omega_k) + (\omega_k - \omega)^2}n(\omega_k, t_{\rm st}). \tag{12}$$

In Eq. (12), the multiplier $\hbar\omega_k\gamma_{\rm rad}(\omega_k)$ indicates how efficiently the quasiparticle shines at the frequency $\omega_k$. As noted above, $\gamma_{\rm rad}(\omega_k) \propto 1/|\varepsilon_{\rm M}(\omega_k) + 2|^2$, that is, the modes whose frequencies are located near the plasmon resonance frequency $\omega_{\rm pl}$ shine most efficiently.

## VI. RADIATION SPECTRUM IN EXACT MODEL

To find the spectrum of NSPL, we solve the complete system of equations using computer simulation of Eqs. (2)–(4). In numerical modeling, a solution to Eqs. (2)–(4) is found for a discrete finite set of frequencies $\{\omega_k\}$. This set is defined according to the formula

$$\omega_k = \omega_{\rm min} + \frac{k-1}{N-1}(\omega_{\rm max} - \omega_{\rm min}), \quad k = 1, ..., N, \tag{13}$$

where to compare to the experiment, we consider the frequency region that covers the plasmon resonance line with the minimum and maximum frequencies $\omega_{\rm min} = 1.5\,{\rm eV}$ and $\omega_{\rm max} = 2.4\,{\rm eV}$, $12\,100\,{\rm cm}^{-1}$, respectively, and the total number of frequencies is $N = 400$. The frequency of the plasmon resonance is taken from the experimental data shown in Sec. II (Fig. 2, blue line), $\omega_{\rm pl} = 1.75\,{\rm eV}$. It is assumed that the external EM field has the frequency $\omega_0 = 1.96\,{\rm eV}$, and the radius of the nanoparticle $R = 50$ nm. Once $n_k^{\rm st}$ are found, we substitute $n_k^{\rm st}$ into Eq. (12) and define the spectrum of NSPL. The results of computer simulation give the mode occupation numbers $n_k^{\rm st}$. To determine the NSPL spectrum, $S_{\rm pl}(\omega)$, these numbers are substituted into Eq. (12). Note that in noble metals, the phonon frequencies forming the allowed band lie inside the region between 0 and $\omega_{\rm ph}^{\rm max}$, which is about several THz [34,35]; therefore, driven oscillations inside the interval $(\omega_{\rm ex} - \omega_{\rm ph}^{\rm max}, \omega_{\rm ex} + \omega_{\rm ph}^{\rm max})$ may be excited. Consequently, instead of a discrete spectrum, we obtain a continuous one, shown in Fig. 2 by the red line.

This spectrum reproduces the main characteristics observed in the experiment: the shape of the plasmon resonance in the low-frequency region and the Gibbs distribution in the high-frequency region. It also reproduces the shape of the SSPNS in the low-frequency region and the Gibbs distribution in the high-frequency region. Note that a direct consequence of Eqs. (2)–(4) is an increase in the intensity of the high-frequency part of the PL spectrum with increasing temperature (see Fig. 5). Such an increase has been observed in experiment [9].

Let us compare experimental and theoretical results. In numerical simulation, we use the constant $G_0$ from Eq. (B9) of Appendix B as a fitting parameter. The best fit shown in Fig. 2 is obtained for $G_0 = 10^{-8}\,{\rm s}^{-1}$. One can see that our model correctly describes both the decrease of the amplitude of the high-frequency part of NSPL spectra that changes according to the Gibbs distribution, $\sim\exp(-h(\omega - \omega_0)/k_BT)$, and the maximum in the low-frequency part of NSPL spectra at the frequency of the plasmon resonance. Note that in experiment,

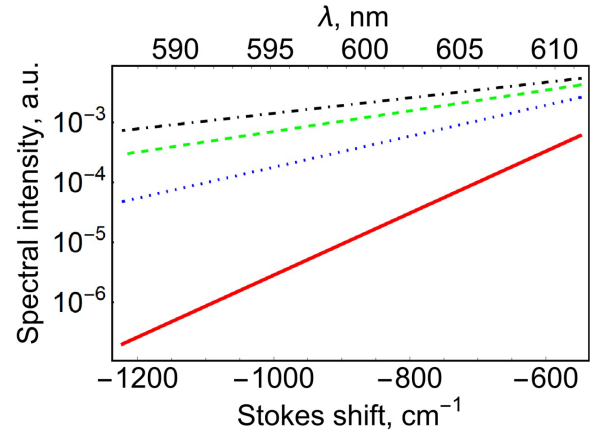


FIG. 5. The high-frequency part of the luminescence spectrum at temperatures 100 K (solid red line), 200 K (dotted blue line), 300 K (dashed green line), and 400 K (dot–dashed black line). For all temperatures, $S(\omega)$ falls off exponentially in agreement with the Gibbs distribution.

the Rayleigh peak in the lower part of the spectrum is usually cut out by a filter, and only the background is visible.

## VII. CONCLUSIONS

The proposed mechanism for PL of nanostructures made of noble metals correctly describes the spectrum for the entire range of frequencies. NSPL is attributed to the cascade Brillouin scattering of the incident wave by metal phonons under the plasmon resonance conditions. The mechanism consists of the cascade Brillouin scattering of the driven oscillation of the electric field inside the SSPNS. The spontaneous Brillouin scattering of the incident EM field excites an oscillation of the EM field inside the nanoparticle at a shifted frequency (the Stokes shift). In turn, the field at the shifted frequency also undergoes Brillouin scattering exciting another oscillation with a lower frequency. This process continues launching a cascade of Brillouin scattering processes of an EM field inside the nanoparticle. The cascade process continues as long as frequencies of new oscillations fall into the SSPNS. In the Stokes part of the spectrum, the developed theory reproduces the SSPNS. We also show that the Gibbs distribution of the high-frequency intensity is due to the anti-Stokes Brillouin scattering. Thus, Brillouin scattering is the inelastic process, the necessity of which has been indicated in Ref. [9]

The developed theory is in good agreement with the experimentally observed NSPL, both below and above the frequency of the incident field. The theory explains the Gibbs distribution of the anti-Stokes component of the NSPL spectrum, which is observed in our experiment. It also describes the increase in the integrated intensity of the anti-Stokes component of the spectrum with increasing metal temperature. In the lower-frequency part of the spectrum, the developed theory reproduces the plasmon resonance line when the plasmon resonance frequency lies below the frequency of the excitation field. In addition, the developed theory reproduces the shift of the maximum of the NSPL spectrum with respect to the plasmon resonant frequency.

NSPL accompanies SERS measurements manifesting itself in the scattering spectrum as a background. This background is superimposed on the SERS signal from the studied molecules, limiting the sensitivity of SERS. The proposed mechanism for NSPL and the microscopic theory of this phenomenon developed in this work show that attempts to increase the SERS accuracy by redesigning substrates by reducing the size of the parts that form hot spots (points of the high-field concentration) should also lead to an increase in the background, which degrades the properties of the substrates. This fact should be taken into account when designing substrates.

## ACKNOWLEDGMENTS

The authors thank I. A. Ryzhikov and I. A. Boginskaya for helpful discussions. The authors also thank Functional Micro/Nanosystem Laboratory from Bauman Moscow State Technical University and G. M. Arzumanyan and K. Mamatkulov for help in organizing and conducting experiments. A.A.L. acknowledges the support of the ONR under Grant No. N00014-20-1-2198. E.S.A. and V.Yu.S. thank the Foundation for the Advancement of Theoretical Physics and Mathematics "Basis."

## APPENDIX A: HAMILTONIAN OF THE SYSTEM

To quantitatively describe the PL spectrum, we quantize the EM field of a plasmon nanoparticle at each frequency of the SSPNS. For this purpose, we use the procedure of macroscopic quantization of EM fields that has been developed for linear media [29,30]. To avoid complicated first-principle calculations [36], the macroscopic quantization does not take into account a complex structure of a medium but only considers the macroscopic response of the medium to an electromagnetic field. This makes it possible to model the medium as a set of elastic quantum dipoles representing oscillation states of electrons [36]. It is assumed that the dipoles interact with the modes of a reservoir. Such a reservoir can be phonons, impurities, etc. The eigenmodes of such a system are the coupled elastic dipoles and reservoir modes. The eigenmodes are found by using the Fano diagonalization procedure [26,30]. The frequencies of these eigenmodes are real, and they differ from the plasmon resonance frequency. The closer the eigenmode frequency to the plasmon resonance frequency, the greater the contribution of the plasmon structure mode into this eigenmode.

At the same time, such a model allows for obtaining permittivity of the medium. The coupling constant between the quantum dipoles with a reservoir is still an unknown free parameter. This parameter can be determined by equating the obtained permittivity to the known permittivity, $\varepsilon_M^{\text{lin}}$, of the metal.

As a result of applying the macroscopic quantization procedure to a metal nanoparticle, it turns out that the eigenmode frequencies fill the SSPNS. The Hamiltonian of such eigenmodes has the form

$$\hat{H}_{\text{pl}} = \sum_k \hbar\omega_k \hat{a}_k^\dagger \hat{a}_k, \tag{A1}$$

where $\hat{a}_k \equiv \hat{a}(\omega_k)$ and $\hat{a}_k^\dagger \equiv \hat{a}^\dagger(\omega_k)$ are the operators of annihilation and creation of the eigenmode with the frequency $\omega_k$. These operators satisfy the Bose commutation relations:

$$[\hat{a}_k, \hat{a}_{k'}^\dagger] = \delta_{kk'}. \tag{A2}$$

Below, for brevity, we use the designation $\hat{a}_k$ instead of $\hat{a}(\omega_k)$. The eigenmodes obtained after the Fano diagonalization are the quasiparticles considered in Refs. [26,30]. The eigenmode is a dressed state consisting of driven oscillations of the field in the nanoparticle and the reservoir modes. The reservoir is responsible for the imaginary part of permittivity or the electron conductivity. For linear phenomena that we consider, this reservoir describes scattering of electrons on impurities in metal and on electrons moving with velocities, which do not contribute to the plasma oscillations.

The operator of the electric near field of the eigenmodes is expressed through the operators $\hat{a}_k$ and $\hat{a}_k^\dagger$ according to

$$\mathbf{E}(\mathbf{r}, t) = \sum_k \mathbf{\Lambda}_k(\mathbf{r})\big(\hat{a}_k^\dagger(t) + \hat{a}_k(t)\big), \tag{A3}$$

where $\mathbf{\Lambda}_k(\mathbf{r})$ are the functions that determine the distribution of the near field created by the eigenmode with the frequency

$\omega_k$. For example, in the dipole approximation, for a spherical subwavelength plasmon particle with the radius $R$ in a vacuum, the function $\mathbf{\Lambda}_k(\mathbf{r})$ has the form [26]

$$\mathbf{\Lambda}_k(\mathbf{r}) = \sqrt{\frac{\hbar\Delta\omega}{\pi R^3\varepsilon_0}}\frac{\sqrt{\mathrm{Im}\varepsilon_{\mathrm{M}}^{(\mathrm{lin})}(\omega_k)}}{\left|\varepsilon_{\mathrm{M}}^{(\mathrm{lin})}(\omega_k)+2\right|} \times \mathbf{e}_z\begin{cases}\mathrm{grad}[(r/R)/2\sqrt{\pi}], & r<R,\\ \mathrm{grad}[3(R/r)^2\cos\theta/2\sqrt{\pi}], & r>R,\end{cases}$$

where $\varepsilon_0$ is the dielectric constant of vacuum, $\Delta\omega$ is the sampling frequency of the SSPNS, the radius-vector $\mathbf{r}$ is expressed in terms of polar, $\theta$, and azimuthal, $\varphi$, angles as $\mathbf{r} = [r\sin\theta\cos\varphi,\ r\sin\theta\sin\varphi,\ r\cos\theta]$, and $\mathbf{e}_z$ is the unit vector in the $z$ direction. Consequently, the dipole moment is directed along the $z$ axis. We emphasize that only the linear part of permittivity $\varepsilon_{\mathrm{M}}^{(\mathrm{lin})}(\omega_n)$ is used in the expression for the plasmon electric-field operator. Below, we take into account that the electric field per one quantum, $\mathbf{\Lambda}_k(\mathbf{r})$, is inversely proportional to the volume of the nanoparticle, $\mathbf{\Lambda}_k(\mathbf{r}) \sim 1/\sqrt{R^3} \sim 1/\sqrt{V}$.

Let us consider the interaction of the nanoparticle with an external monochromatic wave having the frequency $\omega_0$. Due to the monochromatic character of the external field and linearity of the medium, the excited quasiparticle also has the frequency $\omega_0$. This interaction is described by the Hamiltonian $\hat{H}_{\mathrm{ex}}$:

$$\hat{H}_{\mathrm{ex}} = -\hat{\mathbf{d}}_0\cdot\mathbf{E}(\mathbf{r}_{\mathrm{pl}})\cos(\omega_0 t) = \hbar\Omega_{\mathrm{ex}}\hat{a}_0^\dagger e^{-i\omega_0 t} + \mathrm{H.c.}, \quad \text{(A4)}$$

where $\hat{\mathbf{d}}_0 = \mathbf{d}_0(\hat{a}_0^\dagger + \hat{a}_0)$ is the operator of the dipole moment of a quasiparticle with the frequency $\omega_0$, $\Omega_{\mathrm{ex}} = -\mathbf{d}_0\cdot\mathbf{E}(\mathbf{r}_{\mathrm{pl}})/\hbar$ is the Rabi constant of the interaction of the quasiparticle with the external field. The value of the dipole moment $\mathbf{d}_0 \equiv \mathbf{d}(\omega_0)$ is determined by the geometry and permittivity of the nanoparticle.

All quasiparticle dipole moments have the same dependence on the frequency and the nanoparticle radius. For example, the dipole moment, $\mathbf{d}(\omega)$, of a spherical subwavelength plasmon nanoparticle of the radius $R$ in vacuum is determined by the expression [26]

$$\mathbf{d}(\omega) = 4\pi R^3\sqrt{\frac{\Delta\omega\hbar\varepsilon_0}{\pi R^3}}\frac{\sqrt{\mathrm{Im}\varepsilon_{\mathrm{M}}^{(\mathrm{lin})}(\omega)}}{\left|\varepsilon_{\mathrm{M}}^{(\mathrm{lin})}(\omega)+2\right|}\mathbf{e}_d. \quad \text{(A5)}$$

Below, we consider the radiated intensity of a quasiparticle (see Appendix C). The dipole moment is determined by Eq. (A5), and the radiated intensity is proportional to the square of this dipole moment. In the neighborhood of the plasmon resonance, $\omega \approx \omega_{\mathrm{pl}}$, permittivity is proportional to $\sim((\omega-\omega_{\mathrm{pl}})^2+\gamma_{\mathrm{pl}}^2)^{-2}$, where we denote $\gamma_{\mathrm{pl}} = \mathrm{Im}\varepsilon_{\mathrm{M}}^{(\mathrm{lin})}(\omega_{\mathrm{pl}})/(\partial\mathrm{Re}\varepsilon_{\mathrm{M}}^{(\mathrm{lin})}(\omega_{\mathrm{pl}})/\partial\omega)$. This quantity $\gamma_{\mathrm{pl}}$ has the meaning of the width of the SSPNS.

Next, we find the Hamiltonian of the interaction of quasiparticles with phonons in metal, which gives an additional nonlinear part in $\mathrm{Im}\varepsilon_{\mathrm{M}}(\omega_{\mathrm{pl}})$. The electric field inside the medium induces polarization caused by the displacement of electrons from the equilibrium positions. In turn, the electrons' displacement leads to a displacement of nuclei of the crystal lattice. Displaced nuclei excite phonons, which result in the changing local density of the medium. This changing, in turn, affects the dielectric constant of metal [37]. Suppose that at the point $\mathbf{r}$, a nucleus deviates from the equilibrium position by $\mathbf{q}(\mathbf{r})$. We assume that this deviation is small, allowing one to expand the dielectric constant of the metal in the series over $\mathbf{q}(\mathbf{r})$. Retaining the zeroth and the first terms, we obtain

$$\varepsilon(\mathbf{r},\omega) = \varepsilon^{(0)}(\mathbf{r},\omega) + w_i(\omega)q_i(\mathbf{r}), \quad \text{(A6)}$$

where coefficients $w_i(\omega)$ determine the change in the dielectric constant of the metal at the point $\mathbf{r}$ due to the deviation of the nucleus. Substituting Eqs. (A6) and (A3) into the expression for the EM field energy

$$\frac{1}{8\pi}\int_V dV[\partial(\mathrm{Re}(\varepsilon)\omega)/\partial\omega]|\mathbf{E}(\mathbf{r})|^2$$

and retaining the terms proportional to the first order of the nucleus displacement, $q_i(\mathbf{r})$, we obtain the expression for the additional energy of the electric field:

$$\Delta\hat{W} = \frac{1}{8\pi}\int_V d^3\mathbf{r}\tilde{w}_i q_i(\mathbf{r})\left(\mathbf{\Lambda}_n^{(0)*}(\mathbf{r})\hat{a}_n^\dagger + \mathbf{\Lambda}_n^{(0)}(\mathbf{r})\hat{a}_n\right) \times \left(\mathbf{\Lambda}_m^{(0)*}(\mathbf{r})\hat{a}_m^\dagger + \mathbf{\Lambda}_m^{(0)}(\mathbf{r})\hat{a}_m\right), \quad \text{(A7)}$$

where $\tilde{w}_i = \partial(\omega w_i)/\partial\omega$. For simplicity, we suppose that $\tilde{w}_i$ does not depend on $i$, $\tilde{w}_i = \tilde{w}$.

According to the general theory of phonons in metals [37], the operator of the deviation of the $i$ th nucleus from the equilibrium position, $\hat{q}_i$, can be expressed in terms of operators of annihilation, $\hat{b}_k$, and creation, $\hat{b}_k^\dagger$, of the $k$ th phonon mode in the following way:

$$\hat{q}_i(\mathbf{r}) = \sum_l (C_l^*(\mathbf{r})\hat{b}_l^\dagger + C_l(\mathbf{r})\hat{b}_l), \quad \text{(A8)}$$

where operators $\hat{b}_l$ and $\hat{b}_l^\dagger$ obey the commutation relations:

$$[\hat{b}_l, \hat{b}_{l'}^\dagger] = \delta_{l,l'}. \quad \text{(A9)}$$

Functions $C_l(\mathbf{r})$ describe the distribution of the $l$th phonon mode. They satisfy the normalization condition:

$$\int_V d^3\mathbf{r}|C_l(\mathbf{r})|^2 = 1. \quad \text{(A10)}$$

The phonon dynamics is described by the Hamiltonian

$$\hat{H}_{\mathrm{phon}} = \sum_l \hbar\omega_l^{\mathrm{ph}}\hat{b}_l^\dagger\hat{b}_l. \quad \text{(A11)}$$

Substituting Eq. (A8) into Eq. (A7) and discarding the terms proportional to $\hat{a}_n^\dagger\hat{a}_{n'}^\dagger$ and $\hat{a}_n\hat{a}_{n'}$, we reduce the expression for the interaction Hamiltonian of plasmons and phonons to the optomechanical Hamiltonian [28]:

$$\hat{H}_{\text{pl-phon}} = \sum_l\sum_{n,m} w_{nml}(C_l^*(\mathbf{r})\hat{b}_l^\dagger + C_l(\mathbf{r})\hat{b}_l)\hat{a}_n^\dagger\hat{a}_m, \quad \text{(A12)}$$

where $w_{nml}$ are the interaction constants of phonons and plasmons having the form

$$w_{nml} = \tilde{w}\int_V d^3\mathbf{r}\mathbf{\Lambda}_n^{(0)*}(\mathbf{r})\mathbf{\Lambda}_m^{(0)}(\mathbf{r})C_l^*(\mathbf{r}). \quad \text{(A13)}$$

To describe the radiation of the dipole eigenmodes, it is necessary to consider their interaction with free-space modes.

For this purpose, the Hamiltonian of the EM field of a free-space mode is usually introduced:

$$\hat{H}_{\text{rad}} = \sum_{\mu=1,2} \int d^3\mathbf{k}\ \hbar\omega_{\mathbf{k}} \hat{f}^{\dagger}(\mu,\mathbf{k})\hat{f}(\mu,\mathbf{k}). \tag{A14}$$

Here $\omega_{\mathbf{k}} = c|\mathbf{k}|$, $\hat{f}(\mu,\mathbf{k})$ and $\hat{f}^{\dagger}(\mu,\mathbf{k})$ are annihilation and creation operators of the EM field of the free-space mode with the polarization $\mu$ and the wave vector $\mathbf{k}$, satisfying the following commutation relations:

$$[\hat{f}(\mu,\mathbf{k}), \hat{f}^{\dagger}(\mu',\mathbf{k}')] = \delta_{\mu\mu'}\delta(\mathbf{k}-\mathbf{k}'). \tag{A15}$$

The interaction between the dipole moments of the eigenmodes of a nanoparticle and the electric field of the free-space modes has the form

$$\begin{aligned}\hat{H}_{\text{pl-rad}} &= \sum_n -\hat{\mathbf{d}}_n \cdot \hat{\mathbf{E}}_n \\ &= \sum_{\mu=1,2} \int d^3\mathbf{k} \sum_n \hbar\Omega_n(\mu,\mathbf{k})\hat{a}_n^{\dagger}\hat{f}(\mu,\mathbf{k}) + \text{H.c.}\end{aligned} \tag{A16}$$

Here $\Omega_n(\mu,\mathbf{k}) = -\mathbf{d}_n \cdot \mathbf{E}_{\mu,\mathbf{k}}(\mathbf{r})/\hbar$ is the Rabi constant of the interaction of the electric field of the free-space mode with the polarization $\mu$ and the wave vector $\mathbf{k}$ with the eigenmode of the plasmon particle.

Thus, the described system includes plasmons of a subwavelength metal nanoparticle, the external EM wave incident on the nanoparticle, free-space photons, and phonons of the metal nanoparticle. The Hamiltonian of this system is the sum of the Hamiltonians (A1), (A4), (A11)–(A14), and (A16):

$$\hat{H} = \hat{H}_{\text{pl}} + \hat{H}_{\text{phot}} + \hat{H}_{\text{pl-phot}} + \hat{H}_{\text{ex}} + \hat{H}_{\text{phon}} + \hat{H}_{\text{pl-phon}}. \tag{A17}$$

## APPENDIX B: ELIMINATION OF PHONON DEGREES OF FREEDOM IN THE MARKOV APPROXIMATION

Due to the large number of degrees of freedom described by Hamiltonian (A17), it is difficult to find the system eigenmodes even numerically. We, therefore, should make some simplifications. We exclude the degrees of freedom of phonons in metal and free-space photons. After this, instead of considering a closed quantum system, which includes photons, phonons, and EM modes of a sphere excited by an external field, we have to deal with an open quantum system, which only includes the plasmon-polariton modes. Consequently, instead of the Schrödinger equation, it is more convenient to use the master equation for the density matrix.

To obtain the master equation, it is necessary to exclude the photon and phonon subsystems sequentially. Using the standard procedure for excluding the reservoir of free-space modes [33], we obtain the Lindblad superoperator $\hat{L}_{\text{photon}}(\hat{\rho})$, describing the relaxation of the plasmon density matrix $\hat{\rho}$ [33]:

$$\hat{L}_{\text{photon}}(\hat{\rho}) = \sum_n \frac{1}{2}\gamma_{\text{rad}}(\omega_n)\{2\hat{a}_n\hat{\rho}\hat{a}_n^{\dagger} - \hat{\rho}\hat{a}_n^{\dagger}\hat{a}_n - \hat{a}_n^{\dagger}\hat{a}_n\hat{\rho}\}, \tag{B1}$$

where the decay rate $\gamma_{\text{rad}}(\omega_n)$ of the quasiparticle at the frequency $\omega_n$ is determined according to Fermi's golden rule [33]:

$$\gamma_{\text{rad}}(\omega_n) = \pi \sum_{\mu=1,2} \int d^3\mathbf{k}|\Omega_n(\mu,\mathbf{k})|^2\delta(\omega_n - c|\mathbf{k}|). \tag{B2}$$

The rate of quasiparticle energy loss at the frequency $\omega_n$ is determined by the dipole moment of the quasiparticle and is proportional to $\gamma_{\text{rad}}(\omega_n) \propto 1|\varepsilon_{\text{M}}(\omega_n) + 2|^2$ [26]. The Lindblad superoperator (B1) describes the process of quasiparticle energy loss due to radiation into free space [38]. As a result, the term corresponding to the free-space modes is excluded from the Hamiltonian of the whole closed system, but Lindbladian (B1) appears in the master equation:

$$\frac{\partial\hat{\rho}}{\partial t} = \frac{i}{\hbar}[\hat{\rho}, \hat{H}_{\text{pl}} + \hat{H}_{\text{ex}} + \hat{H}_{\text{phon}} + \hat{H}_{\text{pl-phon}}] + \hat{L}_{\text{photon}}[\hat{\rho}]. \tag{B3}$$

Now, we can exclude the phonon subsystem. For this purpose, we assume that phonons are in a state of thermodynamic equilibrium with fixed temperature $T$ at any moment of time. For convenience, in Hamiltonian (A13), we switch to the interaction representation:

$$\begin{aligned}\hat{H}_{\text{pl-phon}} = \sum_l \sum_{n,m} w_{nml}\big(C_l^*(\mathbf{r})\hat{b}_l^{\dagger}e^{i\omega_l^{\text{ph}}t} + C_l(\mathbf{r})\hat{b}_l e^{-i\omega_l^{\text{ph}}t}\big) \\ \times\ \hat{a}_n^{\dagger}e^{i\omega_n t}\hat{a}_m e^{-i\omega_m t}.\end{aligned} \tag{B4}$$

The interaction Hamiltonian of phonons and quasiparticles, Eq. (B4), describes the inelastic process of phonons' absorption/emission. In this process, the energy is transferred from the quasiparticle with the frequency $\omega_n$ to the one with the frequency $\omega_m$. This is the process of Brillouin scattering.

Next, following the standard procedure of the reservoir exclusion [33], in which the phonon subsystem with Hamiltonian (A11) serves as a reservoir, we obtain the Lindblad relaxation superoperator $\hat{L}_{\text{phonons}}(\hat{\rho})$ that describes the relaxation of the density matrix of the plasmon subsystem $\hat{\rho}$:

$$\hat{L}_{\text{phonon}}(\hat{\rho}) = \sum_n \sum_m G_{\omega_m,\omega_n}\{2\hat{a}_n^{\dagger}\hat{a}_m\hat{\rho}\hat{a}_m^{\dagger}\hat{a}_n - \hat{\rho}\hat{a}_m^{\dagger}\hat{a}_n\hat{a}_n^{\dagger}\hat{a}_m - \hat{a}_m^{\dagger}\hat{a}_n\hat{a}_n^{\dagger}\hat{a}_m\hat{\rho}\}. \tag{B5}$$

In Eq. (B5), the function $G(\omega_n - \omega_m)$ is the rate of the relaxation processes, which is determined from Fermi's golden rule [33]:

$$G_{\omega_m,\omega_n} = \begin{cases} \pi\sum_l |w_{nml}|^2\big(1 + N\big(\omega_l^{\text{ph}}\big)\big)\delta\big(\omega_n - \omega_m - \omega_l^{\text{ph}}\big), & \omega_n - \omega_m > 0, \\ \pi\sum_l |w_{nml}|^2 N\big(\omega_l^{\text{ph}}\big)\delta\big(\omega_m - \omega_n - \omega_l^{\text{ph}}\big), & \omega_n - \omega_m < 0. \end{cases} \tag{B6}$$

The function $G_{\omega_m,\omega_n}$ has two important features. First, since above the frequency $\omega^{\rm ph}_{\rm max}$ the density of states of phonons is zero, then

$$G_{\omega_m,\omega_n} = 0, \quad \text{when} \quad \omega_m - \omega_n > \omega^{\rm ph}_{\rm max} \tag{B7}$$

Second, since phonons are in thermodynamic equilibrium with temperature $T$, one obtains

$$G_{\omega_m,\omega_n} \propto \exp\left(-\hbar(\omega_m - \omega_n)/k_B T\right) G_{\omega_n,\omega_m}. \tag{B8}$$

The relaxation operator (B5) reflects the structure of excluded Hamiltonian (A12) and describes Brillouin scattering, in which the quasiparticle with the frequency $\omega_n$ turns into the quasiparticle with the frequency $\omega_m$ due to scattering on the phonon with the frequency $\omega_n - \omega_m$. If $\omega_n - \omega_m > 0$, then the process corresponds to the Stokes scattering, and the energy is absorbed by the phonon reservoir. In the opposite case, $\omega_n - \omega_m < 0$, this is the anti-Stokes scattering, in which the energy of a quasiparticle increases by $\hbar(\omega_m - \omega_n)$. This energy is drawn from the thermal energy of the phonon reservoir. From Eq. (B8) it follows that the speed of the first process is greater than the speed of the second one by the factor of $(1 + N(\omega^{\rm ph}_{\mathbf{k}}))/N(\omega^{\rm ph}_{\mathbf{k}}) = \exp(\hbar\Delta\omega/k_B T)$, so that we have a more intensive excitation of the low-frequency modes.

In Eq. (B6), using the phonon density of states, $D(\omega^{\rm ph})$, the sum over phonon wave vectors can be replaced by the integral over frequencies $\omega^{\rm ph}_l$ as $\sum_l = \int d\omega^{\rm ph} D(\omega^{\rm ph})$. To advance further, we assume that in the frequency range from 0 to $\omega^{\rm ph}_{\rm max}$, phonons have the linear dispersion, $\omega^{\rm ph} = u|\mathbf{k}|$, where $u$ is the speed of sound. In this case, for the density of states, we have $D(\omega^{\rm ph}) = 3V(\omega^{\rm ph})^2/2\pi^2 u^3$ [39]. Then, performing the integration in Eq. (B6) and using the expression for the function $w_{nml}$, Eq. (A13), we obtain

$$\begin{aligned} G_{\omega_m,\omega_n} &= \frac{|w_{nm}(\omega_n - \omega_m)|^2 \hbar^3 \omega_n \omega_m}{2\pi M c^3_{\rm ph}} (\omega_n - \omega_m)(1 + N(\omega_n - \omega_m)) \\ &\times \left( \sin\left(\frac{(\omega_n - \omega_m)R}{v_s}\right) - \frac{(\omega_n - \omega_m)R}{v_s} \cos\left(\frac{(\omega_n - \omega_m)R}{v_s}\right)\right)^2 \left(V k_l^3\right)^{-2} \\ &= G_0(\omega_n - \omega_m)(1 + N(\omega_n - \omega_m)) \left( \sin\left(\frac{(\omega_n - \omega_m)R}{v_s}\right) - \frac{(\omega_n - \omega_m)R}{v_s} \cos\left(\frac{(\omega_n - \omega_m)R}{v_s}\right)\right)^2 \left(V k_l^3\right)^{-2}, \end{aligned} \tag{B9}$$

where $0 \leqslant \omega_n - \omega_m \leqslant \omega^{\rm ph}_{\rm max}$ and we denote $G_0 = (|w_{nm}(\omega_n - \omega_m)|^2 \hbar^3 \omega_n \omega_m)/(2\pi M c^3_{\rm ph})$. In numerical simulation, we use the parameter $G_0$ as a fitting parameter.

Now, we obtain the master equation, from which phonon Hamiltonians (A11) and (B4) are excluded, and which contains a dissipative operator $\hat{L}_{\rm phonon}(\hat{\rho})$:

$$\frac{\partial \hat{\rho}}{\partial t} = \frac{i}{\hbar}[\hat{\rho}, \hat{H}_{\rm pl} + \hat{H}_{\rm ex}] + \hat{L}_{\rm photon}(\hat{\rho}). \tag{B10}$$

Finally, using the identities $\langle \dot{\hat{a}}_k \rangle = {\rm Tr}(\dot{\hat{\rho}}\hat{a}_k) \equiv a_k$ and $\langle \dot{\hat{n}}_k \rangle = {\rm Tr}(\dot{\hat{\rho}}\hat{n}_k) = n_k$, commutation relation (A2), and the master equation for the density matrix, Eq. (B10), we arrive at the equation for the expected value $a_k$ of operators $\hat{a}_k$ and $\hat{n}_k$. For $a_k$ we obtain

$$\begin{aligned} \frac{da_k}{dt} &= \frac{i}{\hbar}{\rm Tr}\left(\hat{a}_k \left[\sum_n \hbar\omega_n \hat{a}^\dagger_n \hat{a} + \hbar\Omega_{\rm ex}\hat{a}^\dagger_0 e^{-i\omega_0 t} + \hbar\Omega_{\rm ex}\hat{a}^\dagger_0 e^{-i\omega_0 t}, \hat{\rho}\right]\right) \\ &+ {\rm Tr}\left(a_k \sum_n \sum_m G_{\omega_m,\omega_n}\left\{2\hat{a}^\dagger_n \hat{a}_m \hat{\rho} \hat{a}^\dagger_m \hat{a}_n - \hat{\rho}\hat{a}^\dagger_m \hat{a}_n \hat{a}^\dagger_n \hat{a}_m - \hat{a}^\dagger_m \hat{a}_n \hat{a}^\dagger_n \hat{a}_m \hat{\rho}\right\}\right) + {\rm Tr}\left(a_k \sum_n \frac{1}{2}\gamma_{\rm rad}(\omega_n)\left\{2\hat{a}_n \hat{\rho} \hat{a}^\dagger_n - \hat{\rho}\hat{a}^\dagger_n \hat{a}_n - \hat{a}^\dagger_n \hat{a}_n \hat{\rho}\right\}\right) \\ &= (-i\omega_k){\rm Tr}(\hat{a}_k\hat{\rho}) - i\Omega_{\rm ex}e^{-i\omega_0 t}\delta_{k,0}{\rm Tr}(\hat{\rho}) + \sum_m G_{\omega_m,\omega_k}{\rm Tr}(\hat{a}_k\hat{n}_m\hat{\rho}) \\ &- G_{\omega_k,\omega_m}{\rm Tr}(\hat{a}_k(\hat{n}_m + 1)\hat{\rho}) - G_{\omega_k,\omega_k}{\rm Tr}(\hat{a}_k\hat{\rho}) - \frac{1}{2}\gamma_{\rm rad}(\omega_k){\rm Tr}(\hat{a}_k\hat{\rho}) \\ &= \left(-i\omega_k - \frac{1}{2}\gamma_{\rm rad}(\omega_k) - G_{\omega_k,\omega_k}\right)a_k - i\Omega_{\rm ex}e^{-i\omega_0 t}\delta_{k,0} + \sum_m \{G_{\omega_m,\omega_k}\langle\hat{a}_k\hat{n}_m\rangle - G_{\omega_k,\omega_m}[\langle\hat{a}_k\hat{n}_m\rangle + \langle\hat{a}_k\rangle]\} \end{aligned} \tag{B11}$$

Further, we take into account that $G_{\omega_k,\omega_k} = 0$ [see Eq. (B9)], and in the mean-field approximation, we uncouple the correlations $\langle\hat{a}_k\hat{n}_m\rangle = \langle\hat{a}_k\rangle\langle\hat{n}_m\rangle$. As a result, we have

$$\frac{da_k}{dt} = \left(-i\omega_k - \frac{1}{2}\gamma_{\rm rad}(\omega_k)\right)a_k - i\Omega_{\rm ex}e^{-i\omega_0 t}\delta_{k,0} + a_k\sum_m \left\{G_{\omega_m,\omega_k}n_m - G_{\omega_k,\omega_m}(n_m + 1)\right\}. \tag{B12}$$

These are Eqs. (2) and (3) from the main text. Similarly, we obtain Eq. (4) for $n_k$, $k \neq 0$:

$$\begin{aligned}\frac{dn_k}{dt} &= \frac{i}{\hbar}\mathrm{Tr}\left(n_k\left[\sum_n \hbar\omega_n \hat{a}_n^\dagger \hat{a} + \hbar\Omega_{\mathrm{ex}}\hat{a}_0^\dagger e^{-i\omega_0 t} + \hbar\Omega_{\mathrm{ex}}\hat{a}_0^\dagger e^{-i\omega_0 t}, \hat{\rho}\right]\right) \\ &+ \mathrm{Tr}\left(n_k \sum_n \sum_m G_{\omega_m,\omega_n}\left\{2\hat{a}_n^\dagger \hat{a}_m \hat{\rho}\hat{a}_m^\dagger \hat{a}_n - \hat{\rho}\hat{a}_m^\dagger \hat{a}_n \hat{a}_n^\dagger \hat{a}_m - \hat{a}_m^\dagger \hat{a}_n \hat{a}_n^\dagger \hat{a}_m \hat{\rho}\right\}\right) \\ &+ \mathrm{Tr}\left(n_k \sum_n \frac{1}{2}\gamma_{\mathrm{rad}}(\omega_n)\left\{2\hat{a}_n \hat{\rho}\hat{a}_n^\dagger - \hat{\rho}\hat{a}_n^\dagger \hat{a}_n - \hat{a}_n^\dagger \hat{a}_n \hat{\rho}\right\}\right) \\ &= \sum_m G_{\omega_m,\omega_k}\mathrm{Tr}((1+\hat{n}_k)\hat{n}_m\hat{\rho}) - G_{\omega_k,\omega_m}\mathrm{Tr}(\hat{n}_k(\hat{n}_m+1)\hat{\rho}) - \gamma_{\mathrm{rad}}(\omega_k)\mathrm{Tr}(\hat{n}_k\hat{\rho}) \\ &\approx -\gamma_{\mathrm{rad}}(\omega_k)n_k + 2\sum_m \left\{G_{\omega_m,\omega_k} n_m[1+n_k] - G_{\omega_k,\omega_m} n_k[1+n_m]\right\}. \end{aligned} \tag{B13}$$

## APPENDIX C: RELATION BETWEEN NUMBERS OF QUASIPARTICLES AND EMITTED PHOTONS

As mentioned in Sec. III, we calculate the PL background as a two-step process. At the first step, we find the number of quasiparticles excited during the cascade process by the external field. The detail of calculations demanded in the first step are described in Appendix B. Here we discuss the second step, in which the number of photons emitted by the given number of quasiparticles is determined.

To find the number of emitted photons, $N(\mu, \mathbf{k}, t) = \hat{f}^\dagger(\mu, \mathbf{k})\hat{f}(\mu, \mathbf{k})$, with the wave vector $\mathbf{k}$ and the polarization $\mu$, we assume that the amplitude $a_m$ is determined by the system of Eq. (B12). Using Hamiltonians (A14) and (A16), we can write the Heisenberg equation for the annihilation operator $\hat{f}(\mu, \mathbf{k})$:

$$\begin{aligned}\dot{\hat{f}}(\mu, \mathbf{k}, t) &= \frac{i}{\hbar}[\hat{H}_{\mathrm{rad}} + \hat{H}_{\text{pl-rad}}, \hat{f}(\mu, \mathbf{k}, t)] \\ &= -i\omega_{\mathbf{k}}\hat{f}(\mu, \mathbf{k}) - i\sum_m \Omega_m(\mu, \mathbf{k})\hat{a}_m(t) \end{aligned} \tag{C1}$$

In Eq. (C1), we assume that the initial moment of time is $t_{\mathrm{st}}$, i.e., the time for which the number of quasiparticle reaches its stationary value, is determined by Eq. (B12). The integration of Eq. (C1) gives

$$\hat{f}(\mu, \mathbf{k}, t) = \hat{f}(\mu, \mathbf{k}, t_{\mathrm{st}})\exp(-i\omega_{\mathbf{k}}\tau) - i\sum_m \Omega_m(\mu, \mathbf{k})\int_0^t d\tau \hat{a}_m(t_{\mathrm{st}} + \tau)\exp(-i\omega_{\mathbf{k}}\tau), \tag{C2}$$

where $t$ is counted from $t_{\mathrm{st}}$. The mean value of the photon number in each EM free-space mode is

$$\begin{aligned} N(\mu, \mathbf{k}, t) &= \langle \hat{f}^\dagger(\mu, \mathbf{k}, t)\hat{f}(\mu, \mathbf{k}, t)\rangle \\ &= \langle \hat{f}^\dagger(\mu, \mathbf{k}, t_{\mathrm{st}})\hat{f}(\mu, \mathbf{k}, t_{\mathrm{st}})\rangle + \sum_m \left(-i\Omega_m(\mu, \mathbf{k})\int_0^t d\tau \langle \hat{f}^\dagger(\mu, \mathbf{k}, t_{\mathrm{st}})\hat{a}_m(t_{\mathrm{st}} + \tau)\rangle e^{i\omega_{\mathbf{k}}\tau} + \mathrm{h.c.}\right) \\ &+ \sum_{m_1, m_2} \Omega_{m_1}(\mu, \mathbf{k})\Omega_{m_2}^*(\mu, \mathbf{k})\int_0^t d\tau_2 \int_0^t d\tau_1 \left\langle \hat{a}_{m_2}^\dagger(t_{\mathrm{st}} + \tau_2)\hat{a}_{m_1}(t_{\mathrm{st}} + \tau_1)\right\rangle \exp(i\omega_{\mathbf{k}}(\tau_1 - \tau_2)). \end{aligned} \tag{C3}$$

In the right-hand part of Eq. (C3), the first term is the number of thermal photons, $\langle \hat{f}^\dagger(\mu, \mathbf{k}, t_{\mathrm{st}})\hat{f}(\mu, \mathbf{k}, t_{\mathrm{st}})\rangle \approx \exp(-\hbar\omega_{\mathbf{k}}/kT)$. At optical frequencies and room temperature, this contribution is much less than unity; below, we neglect it. To evaluate the second term, we use the mean-field approximation, in which the operators of a quasiparticle and free-space photons are uncorrelated, as $\langle \hat{f}^\dagger(\mu, \mathbf{k}, t_{\mathrm{st}})\hat{a}_m(\tau)\rangle \approx \langle \hat{f}^\dagger(\mu, \mathbf{k}, t_{\mathrm{st}})\rangle\langle \hat{a}_m(\tau)\rangle$. Because $\hat{f}^\dagger(\mu, \mathbf{k}, t_{\mathrm{st}})$ is the operator of thermal photons, which are incoherent, we have $\langle \hat{f}^\dagger(\mu, \mathbf{k}, t_{\mathrm{st}})\rangle = 0$. Thus, the second term is zero. To calculate the third term, we substitute the integration variable, $\tau_1$, with $\tau = \tau_1 - \tau_2$, and obtain

$$N(\mu, \mathbf{k}, t) = \sum_{m_1, m_2} \Omega_{m_1}(\mu, \mathbf{k})\Omega_{m_2}^*(\mu, \mathbf{k})\int_0^t d\tau_2 \int_{-\tau_2}^{t-\tau_2} d\tau \langle \hat{a}_{m_2}^\dagger(t_{\mathrm{st}} + \tau_2)\hat{a}_{m_1}(t_{\mathrm{st}} + \tau_2 + \tau)\rangle \exp(i\omega_{\mathbf{k}}\tau). \tag{C4}$$

In Eq. (C4), due to the exponential factor $\exp(i\omega_{\mathbf{k}}\tau)$, the main contribution to the integral over $\tau$ comes from the region near $\tau = 0$. Therefore, we can expand the limits of integration to infinity:

$$N(\mu,\mathbf{k},t) \approx \sum_{m_1,m_2} \Omega_{m_1}(\mu,\mathbf{k})\Omega^*_{m_2}(\mu,\mathbf{k}) \int_0^t d\tau_2 \int_{-\infty}^{\infty} d\tau \left\langle \hat{a}^\dagger_{m_2}(t_{\mathrm{st}}+\tau_2)\hat{a}_{m_1}(t_{\mathrm{st}}+\tau_2+\tau)\right\rangle \exp(i\omega_{\mathbf{k}}\tau). \tag{C5}$$

Further, since we assume that the value of $\hat{a}^\dagger_{m_2}$ reaches its stationary state at the time $t_{\mathrm{st}}$, then at the time $t_{\mathrm{st}}+\tau_2 \geqslant t_{\mathrm{st}}$, the value $\hat{a}^\dagger_{m_2}(t_{\mathrm{st}}+\tau_2)$ is also equal to its stationary state. Therefore, $\hat{a}^\dagger_{m_2}(t_{\mathrm{st}}+\tau_2) = \hat{a}^\dagger_{m_2}(t_{\mathrm{st}})$. Thus, from Eq. (C5) we have

$$\begin{aligned} N(\mu,\mathbf{k},t) &= \sum_{m_1,m_2} \Omega_{m_1}(\mu,\mathbf{k})\Omega^*_{m_2}(\mu,\mathbf{k}) \int_0^t d\tau_2 \int_{-\infty}^{\infty} d\tau \left\langle \hat{a}^\dagger_{m_2}(t_{\mathrm{st}})\hat{a}_{m_1}(t_{\mathrm{st}}+\tau)\right\rangle \exp(i\omega_{\mathbf{k}}\tau) \\ &= t \sum_{m_1,m_2} \Omega_{m_1}(\mu,\mathbf{k})\Omega^*_{m_2}(\mu,\mathbf{k}) \int_{-\infty}^{\infty} d\tau \left\langle \hat{a}^\dagger_{m_2}(t_{\mathrm{st}})\hat{a}_{m_1}(t_{\mathrm{st}}+\tau)\right\rangle \exp(i\omega_{\mathbf{k}}\tau). \end{aligned} \tag{C6}$$

In the mean-field approximation, it is implied that the operators of quasiparticles at different frequencies do not correlate $\langle \hat{a}^\dagger_{m_2}(t_{\mathrm{st}})\hat{a}_{m_1}(t_{\mathrm{st}}+\tau)\rangle \approx \langle \hat{a}^\dagger_{m_2}(t_{\mathrm{st}})\rangle\langle \hat{a}_{m_1}(t_{\mathrm{st}}+\tau)\rangle$ for $m_1 \neq m_2$. Since excitations of quasiparticles arise due to incoherent Brillouin scattering, $\langle \hat{a}^\dagger_{m_2}(t_{\mathrm{st}})\rangle = 0$. Therefore, in Eq. (C6), only the terms with $m_1 = m_2$ give nonzero contributions:

$$\begin{aligned} N(\mu,\mathbf{k},t) = t \sum_m |\Omega_m(\mu,\mathbf{k})|^2 \int_{-\infty}^{\infty} d\tau \langle \hat{a}^\dagger_m(t_{\mathrm{st}})\hat{a}_m(t_{\mathrm{st}}+\tau)\rangle \\ \times \exp(i\omega_{\mathbf{k}}\tau). \end{aligned} \tag{C7}$$

To obtain the radiation spectrum, i.e., the energy emitted at the frequency $\omega$, it is necessary to sum $N(\mu,\mathbf{k},t)$ over wave vectors and the polarizations for which $|\mathbf{k}| = \omega/c$:

$$\begin{aligned} S(\omega) &= \hbar\omega \sum_{\substack{\mu,\mathbf{k},\\ |\mathbf{k}|=\omega/c}} N(\mu,\mathbf{k},t) \\ &= \hbar\omega t \sum_m \int_{-\infty}^{\infty} d\tau \left\langle \hat{a}^\dagger_m(t_{\mathrm{st}})\hat{a}_m(t_{\mathrm{st}}+\tau)\right\rangle \exp(i\omega\tau) \\ &\quad \times \sum_{\substack{\mu,\mathbf{k},\\ |\mathbf{k}|=\omega/c}} |\Omega_m(\mu,\mathbf{k})|^2. \end{aligned} \tag{C8}$$

According to Fermi's golden rule, the value $\sum_{\substack{\mu,\mathbf{k},\\ |\mathbf{k}|=\omega/c}} |\Omega_m(\mu,\mathbf{k})|^2$ is equal to $\gamma_{\mathrm{rad}}(\omega_m)/\pi$, where $\gamma_{\mathrm{rad}}(\omega_m)$ is the rate of radiation losses of the quasiparticle with the frequency $\omega_m$. Thus, we arrive at the equation

$$\begin{aligned} S(\omega) = \frac{1}{\pi}\hbar\omega t \sum_m \gamma_{\mathrm{rad}}(\omega_m) \int_{-\infty}^{\infty} d\tau \langle \hat{a}^\dagger_m(t_{\mathrm{st}})\hat{a}_m(t_{\mathrm{st}}+\tau)\rangle \\ \times \exp(i\omega\tau), \end{aligned} \tag{C9}$$

which is equivalent to Eq. (5) from the main text.

Equation (C9) can be expressed through the dipole moment of a nanoparticle. To do this, we return to Eq. (C8), keeping in mind that the Rabi constant of the interaction between a quasiparticle and a free-space photon is equal to $\Omega_m(\mu,\mathbf{k}) = -\mathbf{d}_m \cdot \mathbf{E}_{\mu,\mathbf{k}}(\mathbf{r})/\hbar$. Here $\mathbf{d}_m$ is the matrix element of the quasiparticle dipole moment at the frequency $\omega_m$ and $\mathbf{E}_{\mu,\mathbf{k}}(\mathbf{r}) = \sqrt{2\pi\hbar\omega_{\mathbf{k}}/V}\,\mathbf{e}_{\mu,\mathbf{k}}\exp(i\mathbf{k}\mathbf{r}_{\mathrm{NP}})$ is the vacuum electric field at the nanoparticle location $\mathbf{r}_{\mathrm{NP}}$. The substitution of these expressions in Eq. (C8) gives

$$\begin{aligned} S(\omega) = \hbar\omega t \sum_m \sum_{\substack{\mu,\mathbf{k},\\ |\mathbf{k}|=\omega/c}} \left| \sqrt{\frac{2\pi\omega_{\mathbf{k}}}{V\hbar}}\,\mathbf{e}_{\mu,\mathbf{k}} \cdot \mathbf{d}_m \right|^2 \\ \times \int_{-\infty}^{\infty} d\tau \langle \hat{a}^\dagger_m(t_{\mathrm{st}})\hat{a}_m(t_{\mathrm{st}}+\tau)\rangle \exp(i\omega\tau). \end{aligned} \tag{C10}$$

Thus, the radiation spectrum is proportional to the square of the quasiparticle dipole moment.


[1] A. Mooradian, Phys. Rev. Lett. **22**, 185 (1969).
[2] G. T. Boyd, Z. H. Yu, and Y. R. Shen, Phys. Rev. B **33**, 7923 (1986).
[3] M. B. Mohamed, V. Volkov, S. Link, and M. A. El-Sayed, Chem. Phys. Lett. **317**, 517 (2000).
[4] O. P. Varnavski, M. B. Mohamed, M. A. El-Sayed, and T. Goodson, J. Phys. Chem. B **107**, 3101 (2003).
[5] P. Apell, R. Monreal, and S. Lundqvist, Phys. Scr. **38**, 174 (1988).
[6] M. R. Beversluis, A. Bouhelier, and L. Novotny, Phys. Rev. B **68**, 115433 (2003).
[7] E. Dulkeith, T. Niedereichholz, T. A. Klar, J. Feldmann, G. von Plessen, D. I. Gittins, K. S. Mayya, and F. Caruso, Phys. Rev. B **70**, 205424 (2004).
[8] K.-Q. Lin, J. Yi, J.-H. Zhong, S. Hu, B.-J. Liu, J.-Y. Liu, C. Zong, Z.-C. Lei, X. Wang, and J. Aizpurua, Nat. Commun. **8**, 14891 (2017).
[9] J. T. Hugall and J. J. Baumberg, Nano Lett. **15**, 2600 (2015).
[10] Y. He, J.-J. Li, and K.-D. Zhu, J. Opt. Soc. Am. B **29**, 997 (2012).
[11] D. A. Weitz, T. J. Gramila, A. Z. Genack, and J. I. Gersten, Phys. Rev. Lett. **45**, 355 (1980).
[12] S. Garoff, D. A. Weitz, T. J. Gramila, and C. D. Hanson, Opt. Lett. **6**, 245 (1981).
[13] D. A. Weitz, S. Garoff, C. D. Hanson, T. J. Gramila, and J. I. Gersten, Opt. Lett. **7**, 89 (1982).
[14] J. Kabuss, A. Carmele, T. Brandes, and A. Knorr, Phys. Rev. Lett. **109**, 054301 (2012).

[15] M. Reitz, C. Sommer, and C. Genes, Phys. Rev. Lett. **122**, 203602 (2019).
[16] V. Y. Shishkov, E. S. Andrianov, A. A. Pukhov, A. P. Vinogradov, and A. A. Lisyansky, Phys. Rev. Lett. **122**, 153905 2019).
[17] M. Born and R. Oppenheimer, in *Quantum Chemistry: Classic Scientific Paper* (World Scientific, Singapore, 2000), p.1.
[18] A. Lombardi, M. K. Schmidt, L. Weller, W. M. Deacon, F. Benz, B. de Nijs, J. Aizpurua, and J. J. Baumberg, Phys. Rev. X **8**, 011016 (2018).
[19] P. Roelli, C. Galland, N. Piro, and T. J. Kippenberg, Nat. Nanotechnol. **11**, 164 (2016).
[20] S. Dey, M. Banik, E. Hulkko, K. Rodriguez, V. Apkarian, M. Galperin, and A. Nitzan, Phys. Rev. B **93**, 035411 (2016).
[21] M. Galperin and A. Nitzan, Phys. Rev. B **84**, 195325 (2011).
[22] V. I. Fabelinsky, D. N. Kozlov, S. N. Orlov, Y. N. Polivanov, I. A. Shcherbakov, V. V. Smirnov, K. A. Vereschagin, G. M. Arzumanyan, K. Z. Mamatkulov, and K. N. Afanasiev, J. Raman Spectrosc. **49**, 1145 (2018).
[23] H. J. Carmichael, *Statistical Methods in Quantum Optics 1: Master Equations and Fokker-Planck Equations* (Springer Science & Business Media, Berlin, 2013).
[24] L. Mandel and E. Wolf, *Optical Coherence and Quantum Optics* (Cambridge University Press, Cambridge, 1995).
[25] M. O. Scully and M. S. Zubairy, *Quantum Optics* (AAPT, College Park, MD, 1999).
[26] V. Y. Shishkov, E. S. Andrianov, A. A. Pukhov, and A. P. Vinogradov, Phys. Rev. B **94**, 235443 (2016).
[27] O. Klein, Z. Phys. **41**, 407 (1927).
[28] A. Yariv, *Quantum Electronics*, 3rd ed. (Wiley, New York, 1989).
[29] B. Huttner and S. M. Barnett, Phys. Rev. A **46**, 4306 (1992).
[30] T. G. Philbin, New J. Phys. **12**, 123008 (2010).
[31] A. Penzkofer, A. Laubereau, and W. Kaiser, Progr. Quant. Electron. **6**, 55 (1979).
[32] L. F. Mollenauer, J. C. White, and C. R. Pollock, *Tunable Lasers* (Springer, Berlin, 1992).
[33] H.-P. Breuer and F. Petruccione, *The Theory of Open Quantum Systems* (Oxford University Press, Oxford, 2002).
[34] W. Drexel, W. Gläser, and F. Gompf, Phys. Lett. A **28**, 531 (1969).
[35] J. Lynn, H. Smith, and R. Nicklow, Phys. Rev. B **8**, 3493 (1973).
[36] W. Vogel and D.-G. Welsch, *Quantum Optics* (Wiley, Weinheim, 2006).
[37] R. P. Feynman, *Statistical Mechanics* (Benjamin, CA, 1972).
[38] Y. E. Lozovik, I. A. Nechepurenko, E. S. Andrianov, A. V. Dorofeenko, A. A. Pukhov, and N. M. Chtchelkatchev, Phys. Rev. B **94**, 035406 (2016).
[39] L. D. Landau and E. M. Lifshitz, *Statistical Physics* (Pergamon Press, Fairview Park, NY, 1980), Part 1: Vol. 5.